

Etoposide Model-Induced Changes in Antioxidant Studies Histological and Ultrastructural Evaluations of Hepatic, Renal, and Cardiac Tissues of Male Rats

Cambios Inducidos por el Modelo de Etoposido en Estudios de Antioxidantes, Evaluaciones Histológicas y Ultraestructurales de Tejidos Hepáticos, Renales y Cardíacos de Ratas Macho

Said M.R.Kewedar^{1,2} & Nael Abutaha³

KEWEDAR, S. M. R. & ABUTAHA, N. Etoposide model-induced changes in antioxidant studies histological and ultrastructural evaluations of hepatic, renal, and cardiac tissues of male rats. *Int. J. Morphol.*, 42(3):663-672, 2024.

SUMMARY: Etoposide is an effective antimitotic and antineoplastic agent used to treat various human malignancies. In the present study, Etoposide was injected intraperitoneally into the rats at 1 mg/kg/day for 52 days (52 doses). The control animals received physiological saline (0.5 ml) intraperitoneally daily for 52 doses. The body weight of etoposide-treated rats was significantly reduced compared to control rats. Lipid peroxidation demonstrated an insignificant rise in hepatic tissue, a non-significant decline in renal tissue, and a significant reduction in cardiac tissue. The levels of GSH in hepatic and renal tissue were found to be non-significantly increased but significantly increased in cardiac tissue compared to controls. GR activity was found to be considerably decreased in the treated group. G-S-T levels increased significantly in all treated group. Etoposide injections caused a non-significant change in the GPX level of hepatic tissue, whereas renal and cardiac tissues showed a significant increase. The activity of CAT in hepatic tissue was significantly increased, while CAT activity in renal tissue showed a non-significant decrease, whereas in cardiac tissue, significantly lower levels were observed than in control group. The level of CYTp450 in hepatic and cardiac tissues showed a significant increase; however, renal tissue showed non-significant depletion, whereas CYTb5 in hepatic, renal, and cardiac tissues was significantly lower than controls. The protein content in the hepatic tissue was not significantly increased, whereas the total protein in the renal and cardiac tissues was increased significantly. The research finding is indicative of detoxification activity in the etoposide model.

KEY WORDS: Etoposide; Antioxidant; Histological; Ultrastructural; Hepatic.

INTRODUCTION

Etoposide is a semi-synthetic glycoside derivative of Podophyllotoxin derived from *Podophyllum peltatum* or *Podophyllum emodi* plants (Stähelin & von Wartburg, 1991). Chemotherapeutic agents are either used singly or in combination for cancer treatments. Etoposide is employed in chemotherapy to treat various malignancies such as testicular cancer, lymphoma, acute leukemia, and, small cell lung cancer often administered as a standalone therapeutic agent. Etoposide and cisplatin (or carboplatin) are standard for lung cancer therapy. This medication stands out as one of the most potent plant-derived substances ever examined for its efficacy against murine leukemia (L1210). It demonstrated curative properties, particularly effective in cases of low tumor burdens. Etoposide, one of the

constituents of standard therapeutic regimens, has been reported in combination with doxorubicin, cisplatin, 4-hydroxycyclophosphamide, and vindesine (Henwood & Brogden, 1990). *In vitro*, combining Etoposide and Mafosfamide kill various malignant cell lines from human bone marrow (Henwood & Brogden, 1990). The epipodophyllotoxins, specifically etoposide (VP-16) introduced in 1966 and teniposide (VM-26) in 1967, were in clinical use well before their mechanisms of action were fully comprehended. This class also encompasses several novel derivatives that are currently emerging (Long, 1992).

Etoposide is classified under class III, called "topoisomerase inhibitors." In its lowest energy state, double-

¹ The Pennsylvania State University, State College, PA, USA.

² Department of Life Sciences, University of Mumbai, India.

³ Department of Zoology, College of Science, King Saud University, P.O. Box 2455 Riyadh 11451, Saudi Arabia.

FUNDED: Researchers Supporting Project number (RSPD2024R757), King Saud University, Riyadh, Saudi Arabia.

stranded DNA can be two loosely wound (negatively supercoiled) or two tightly wound (positively supercoiled) (Liu *et al.*, 1980). Topoisomerase, an enzyme, plays a vital role in the replication process by temporarily cleaving one strand, passing the other through the break, and reattaching the cut ends together. Etoposide exerts its effect by hindering the capacity of topoisomerase enzymes to reconnect separated DNA ends, resulting in widespread DNA strand breaks in actively dividing cells. This disruption ultimately triggers a process leading to cell death. It was the first anticancer drug to be demonstrated to work through inhibition of topoisomerase II (Baldwin & Osheroff, 2005).

The recently introduced etopho (etoposide phosphate) offers a significant advantage due to its enhanced solubility in water. Etopophos serves as a prodrug of Etoposide. Following administration, the phosphate group undergoes hydrolysis within the human body, yielding bioactive Etoposide. The hydrophilic nature of etopophos allows for more efficient administration (Witterland *et al.*, 1996). Presently, several new derivatives of Etoposide are undergoing clinical phase studies. For instance, NK611 exhibits improved water solubility and topoisomerase II blocking activity (Hanuske *et al.*, 1995; Mross *et al.*, 1996). TOP 53 and GL 311 stand out as highly promising derivatives, aiming to enhance biological activities with the goal of surpassing the potency of Etoposide and evolving into more effective drugs.

The effect of the anticancer drug on a small test animal such as a rat shows significance in understanding the mechanism of toxicity on various organs such as the liver, kidneys, and heart. The study of the enzymatic and non-enzymatic action of Etoposide on these organs, as well as the changes in the organelles caused by the anticancer drug Etoposide's action using electron microscopy and light microscopy, would help understand the mechanism of toxicity of this anticancer drug.

MATERIAL AND METHOD

Animals. Male albino rats of the Wistar strain, with an average body weight of 240-250 g, were procured from the Haffkines Research Institute in Mumbai, India. These rats were then divided into one control group and one treated group, each comprising five animals. The study received approval from the Institutional Animal Ethical Committee. In the experimental group, rats were subjected to intraperitoneal (i.p.) injections of 1 mg of Etoposide (FYTOSID, Dabur India Ltd) per kilogram daily for 52 days, with some modifications (Mittal *et al.*, 2001). The control group received intraperitoneal injections of 0.5 ml of physiological saline daily for the same duration (52 doses).

The body weights of both the control and etoposide-treated groups were documented weekly throughout the experiment. Simultaneously, the overall health conditions of the rats were closely observed and recorded. After the completion of the treatment, the rats were maintained under consistent laboratory conditions for 2-3 days. Prior to dissection, the animals were anesthetized. Following euthanasia, organs such as the liver, kidney, and heart were extracted. Adherent fat in these tissues was carefully removed and rinsed with chilled normal saline (0.85 %). Subsequently, the tissues were blotted, weighed, and prepared for structural and biochemical studies.

Biochemical examination

Homogenate preparation. A 10 % homogenate was prepared by combining 0.5 g of tissue with 5 ml of 0.1 M sodium phosphate buffer (pH 8.0). The homogenate underwent centrifugation at 9000 rpm for 20 minutes, resulting in the extraction of the supernatant fraction. This supernatant fraction was then utilized to assess antioxidant enzymes.

Samples treated with 25 % and 5 % trichloroacetic acid (TCA) were employed to determine the levels of reduced glutathione and lipid peroxidation. Microsomal fractions, obtained following centrifugation at 105,000 g, were utilized for the estimation of cytochrome P450 and cytochrome b5 enzymes.

Total protein Assessment. The determination of total proteins in tissues was conducted following the protocol outlined by Lowry *et al.* (1951). A calibration curve using bovine serum albumin (BSA) standards was employed to quantify the protein concentration in the samples.

Evaluation of tissue antioxidant status. The thiobarbituric acid (TBA) assay, as outlined by Esterbauer & Cheeseman (1990), was employed to determine the concentration of malondialdehyde (MDA) in 10 % homogenates of the liver, kidney, and heart. Reduced Glutathione (GSH) levels were estimated using the method developed by Moron *et al.* (1979). Glutathione Peroxidase (GPx) (EC 1: 11:9) activity was measured according to the method described by Rotruck *et al.* (1973). Glutathione Reductase (GR) (EC 1.6.4.2) was quantified in hepatic, renal, and cardiac tissues using the procedure outlined by Racker (1955). Catalase (CAT) (EC 1.11.1.6) activity was assessed as per the method by Aebi (Hadwan & Abed, 2016).

Drug Metabolizing Enzymes Activities. Glutathione-S-Transferase G-S-T (EC 2.5.18) was assessed using the method of Habig *et al.* (1974), Cytochrome P450 (CYTp450), Cytochrome b5 (CYTb5) CYTp450 (EC

14.14.1) and CYTb5 (EC 1.6.2.2) were assessed following the methods of Omura & Sato (1964).

Histological examination

Light Microscopy. The animals were humanely euthanized under anaesthesia by dislocating the cervical vertebrae. The hepatic and renal tissues were collected and preserved in Bouin's fixative, following a previously established protocol (Weisel, 1979). Multiple cross-sections were generated from the control and treated groups. These histological sections were prepared utilizing a rotary microtome (Microm, Model No. HM 310), stained with hematoxylin and eosin (H&E), and then observed under a microscope (Leica, Germany). Photographs were taken for documentation.

Transmission electron microscopy. The liver and kidney tissues were dissected from the rats, cut into 1 mm sections, and immersed in a drop of 3 % glutaraldehyde. Subsequently, they were submerged in a fresh, cold fixative for two hours and then transferred to 0.1 M cacodylate buffer for an additional 4 hours. After a brief rinse in the buffer, the tissues underwent post-osmication in 1 % osmic acid for 1 to 2 hours. Following this, a series of increasing alcohol concentrations, propylene oxide, and eventual embedding in resin were used for dehydration. Resin polymerization occurred at 60°C. The blocks were prepared using araldite, and 1 mm sections were cut with a glass knife using an LKB-2000S ultramicrotome. These sections were affixed to glass slides and stained with buffered toluidine blue. The light microscope was employed for area selection, and ultrathin sections of chosen blocks were cut with a diamond knife. These sections were then affixed to copper grids, stained with uranium acetate and lead citrate, and prepared for final examination. Scanning and photography of the ultrathin sections were performed using a JEM-JEOL L00S electron microscope.

Statistical analysis. Data are expressed as mean \pm SEM to compare the groups (Control and Etoposide); a student "t" test was performed. Significance was obtained when $p < 0.05$.

RESULTS

General Observation. No injuries were observed at the injection site in both the treated and control groups. However, in the Etoposide-treated rats, body weight was significantly lower than in the control rats after 8 weeks of intraperitoneal injections (52 doses at 1.0 mg/kg/day). Heart, kidney, and Liver weights of the anticancer drug-treated rats showed non-significant changes compared to the control group (Table I).

Table I. Alterations in body weight and organ weight of male rats due to etoposide administration (mean \pm SEM).

| Parameter | Groups | |
|-------------------|-------------------|-------------------|
| | Control | Etoposide |
| Body weight (g) | 443 \pm 4.35 | 330 \pm 18.5* |
| Liver weight (g) | 11.46 \pm 0.65 | 12.286 \pm 0.79 |
| Kidney weight (g) | 1.261 \pm 0.045 | 1.168 \pm 0.026 |
| Heart weight (g) | 0.928 \pm 0.045 | 0.826 \pm 0.017 |

*Indicates a significant deviation from control values ($p < 0.05$).

Effect of Etoposide on hepatic of male rats. Following eight weeks of etoposide injections, the MDA, GSH, GPx, activities and total protein concentration levels in hepatic tissue exhibited a non-significant increase or decrease compared to the control group. However, the activity of G-S-T, CAT, and CYTp450 in hepatic tissue was significantly higher in treated group compared to the saline-treated group. In contrast, the levels of GR and CYT-b5 in hepatic tissue were significantly decreased in the group compared to the control group (Table II).

Effect of Etoposide on the liver of male rats. After eight weeks of etoposide injections, the levels of MDA, GSH, and GPx activities and total protein contents in liver tissue showed non-significant changes compared to the control group. However, the activities of G-S-T, CAT, and CYTp450 levels in kidney tissue were significantly higher in the etoposide-treated rats than in the saline-treated rats. In contrast, the GR, GPx, and CYTb5 levels in liver tissue were significantly decreased in the treated group compared to the control (Table I).

Table II. Impact of Etoposide on hepatic antioxidant levels, antioxidant enzymes, and total protein in male rats (mean \pm SEM).

| Parameter | Groups | |
|---|---------------------|--------------------|
| | Control | Etoposide |
| Protein (mg/g tissue) | 371.06 \pm 14.927 | 375.86 \pm 10.23 |
| LPXn (nmoles of MDA formed/mg protein) | 0.20 \pm 0.02 | 0.293 \pm 0.021 |
| GSH (μ mols/mg protein) | 13.8 \pm 1.3 | 13.818 \pm 0.91 |
| G-S-T (η mols of CDNB bound/ min/mg protein) | 6.3 \pm 0.4 | 20.66 \pm 1.18* |
| GR (η mols of NADPH red/ min/ mg protein) | 5.0 \pm 0.4 | 2.879 \pm 0.19* |
| GPx (μ g of GSH utilized/ min/mg protein) | 269 \pm 24.06 | 267.76 \pm 26.8 |
| CAT (units /mg protein) | 0.02 \pm 0.00 | 0.07 \pm 0.005* |
| CYTp450 (nmoles of CO bound /mg protein) | 444 \pm 37.46 | 656.99 \pm 31.7* |
| CYTb5 (nmoles of CO bound /mg protein) | 615 \pm 37.0 | 475.53 \pm 42.4* |

*Indicates a significant deviation from the control values ($p < 0.05$).

Effect of Etoposide on the renal of male rats. Following eight weeks of etoposide injections, the MDA, GSH, G-S-T, CAT, and CYTp450 levels in renal tissue exhibited non-significant changes compared to the control group. The specific data can be found in Table II. However, the concentration of protein and GPx in renal tissue was

significantly higher in the etoposide-treated rats than in the saline-treated rats. In contrast, the levels of GR and CYTb5 in renal tissue were significantly decreased in the Etoposide-treated group compared to the control group. The relevant data is available in Table III.

Table III. Impact of Etoposide on renal antioxidant enzymes and total protein in male rats (mean \pm SEM).

| Parameter | Groups | |
|---|---------------------|----------------------|
| | Control | Etoposide |
| Protein (mg/g tissue) | 262.73 \pm 17.356 | 325.27 \pm 19.11 * |
| LPXn (nmoles of MDA formed/mg protein) | 0.31 \pm 0.03 | 0.258 \pm 0.015 |
| GSH (μ mole/mg protein) | 8.06 \pm 0.74 | 7.724 \pm 0.732 |
| G-S-T (η mole of CDNB bound/ min/mg protein) | 1.46 \pm 0.11 | 6.355 \pm 0.35 |
| GR (η mole of NADPH red/ min/ mg protein) | 9.98 \pm 0.37 | 8.304 \pm 0.611* |
| GPx (μ g of GSH utilized/ min/mg protein) | 415.4 \pm 25.14 | 565.76 \pm 29.5* |
| CAT (units /mg protein) | 0.6 17 \pm 0.09 | 0.533 \pm 0.052 |
| CYTp450 (nmoles of CO bound /mg protein) | 683.4 \pm 40.5 | 681.18 \pm 66.95 |
| CYTb5 (nmoles of CO bound /mg protein) | 2605.5 \pm 259.2 | 555.81 \pm 49.57* |

*Indicates a significant deviation from the control values ($p < 0.05$).

Effect of Etoposide on the heart of male rats. Compared to the control group, Etoposide-treated cardiac tissue showed a marked decrease in lipid peroxidation, GR, CAT activities, total protein contents, and CYTb5 levels. Conversely, GSH,

G-S-T, GPx activities, and CYTp450 levels in cardiac tissue significantly increased in the Etoposide-treated group compared to the control group. The relevant data can be found in Table IV.

Table IV. Influence of Etoposide on cardiac antioxidant enzymes and protein profile in male rats (mean \pm SEM).

| Parameter | Groups | |
|---|--------------------|---------------------|
| | Control | Etoposide |
| Protein (mg/g tissue) | 334.26 \pm 13.12 | 287.77 \pm 14.25* |
| LPXn (nmoles of MDA formed/mg protein) | 47.451 \pm 1.70 | 0.037 \pm 0.00* |
| GSH (μ mole/mg protein) | 3.32 \pm 0.31 | 4.33 \pm 0.15* |
| G-S-T (η mole of CDNB bound/ min/mg protein) | 1.715 \pm 0.157 | 2.36 \pm 0.06* |
| GR (η mole of NADPH red/ min/ mg protein) | 0.876 \pm 0.051 | 0.80 \pm 0.03* |
| GPx (μ g of GSH utilized/ min/mg protein) | 379.79 \pm 33.34 | 538.49 \pm 32.92* |
| CAT (units /mg protein) | 7.276 \pm 0.33 | 0.0544 \pm 0.003* |
| CYTp450 (nmoles of CO bound /mg protein) | 25 \pm 0.24 | 8 .0 \pm 0.37* |
| CYTb5 (nmoles of CO bound /mg protein) | 88 \pm 0.4 | 71.0 \pm 0.3* |

*Indicates a significant deviation from the control values ($p < 0.05$).

Light and Electron Microscopic Study

Liver. Structural changes in parenchymal cells were observed under a light microscope. Filled and dilated sinusoidal spaces were noticed in the treated group (Fig. 1A and B). In electron microscopic study, the accumulation of smooth endoplasmic reticulum and numerous dense mitochondrial agglutinations was observed in most hepatocytes, accompanied by the buildup of lipid droplets. These observations suggest heightened detoxification activity in the group treated with etoposide (Fig. 2).

Kidney. Following Etoposide treatment, the glomeruli in the kidney exhibited a markedly distorted structure, and there was an observable increase in the weight of the epithelium lining and the proximal tubule, characterized by narrow lumens. These alterations were discerned under light microscopy (Fig.1 C and D). Electron micrographs following Etoposide treatment unveiled several changes in the ultrastructure of the kidney, reflecting notable damage to the cytoarchitecture. Notable observations included electron-

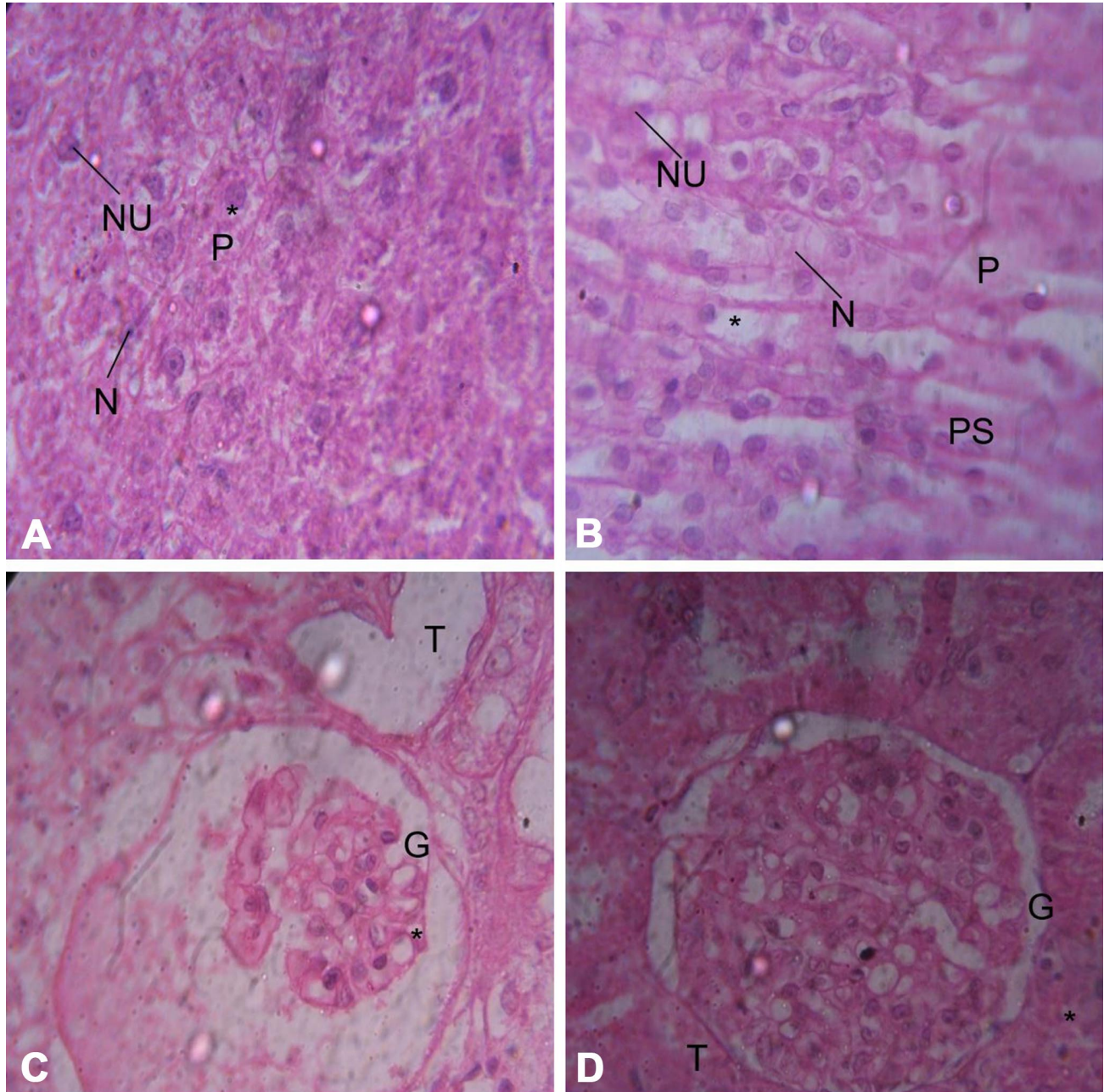


Fig. 1. A-D: Microscopic images of rat liver and kidney sections from experimental groups, stained with Haematoxylin & Eosin. A and B: In the treated group, examinations of liver sections unveil sporadic ruptures in parenchymal (P) tissue accompanied by vacuolations. The portal spaces (PS) appear narrowed, and the central biliary duct (CBD) exhibits amorphous material in the lumen. (Magnification x20). C and D: Sections of the kidneys in the treated group exhibit dilated proximal convoluted tubules (PCT) characterized by an enlarged lumen (L) and vacuolation (*) in the epithelium surrounding the nucleus (N). The nuclei show signs of necrosis, and there is evidence of atrophied glomerulus (G). Additionally, large vacuoles (*) are present in the tubular epithelium, and there is an acute loss of the brush border of the tubules (thin arrow). (Magnification x40).

dense deposits along the epithelial side of the basal membrane, discontinuity in foot processes, and large dilated cisternae of smooth endoplasmic reticula. Additionally, electron micrographs depicted numerous and elongated

mitochondria in the S1 and S2 segments of the proximal tubule. Furthermore, the height of stereocilia in the S2 segment was reduced (Fig. 3).

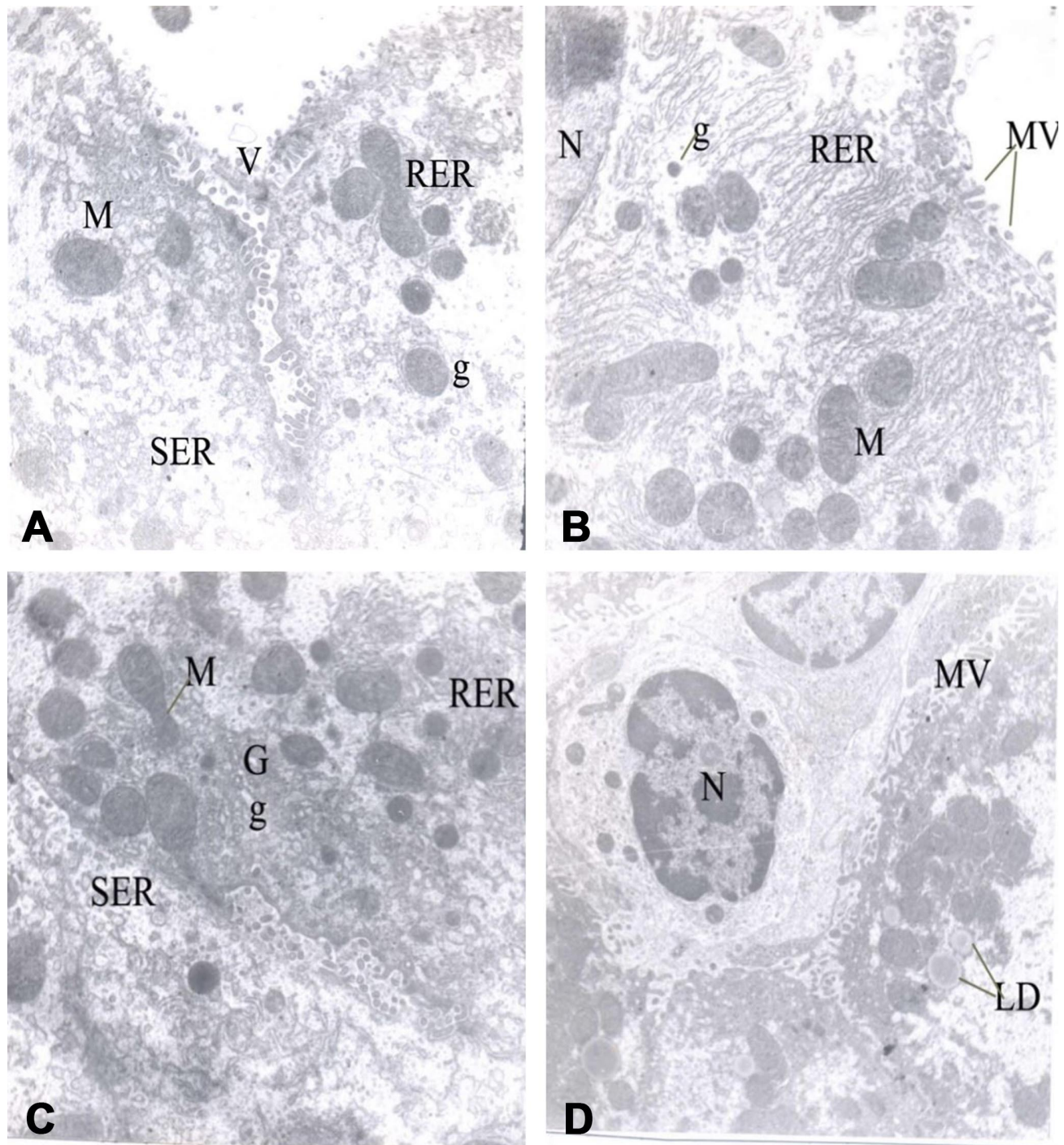


Fig. 2. A: Transmission electron micrograph (TEM) of ultrathin sections of rat hepatocytes. The electron micrograph reveals highly dilated cisternae of smooth endoplasmic reticulum (SER) containing amorphous material. B: The cytoplasm displays accumulations of large mitochondria (M) with a dense matrix and intact, tubular cristae. Numerous tubular laminar cisternae of rough endoplasmic reticulum (RER) are evident. C: A large accumulation of mitochondria (M) with a dense matrix is observed in one instance, alongside a cell with a small but active Golgi apparatus (G) and occasional secretory granules (g), as well as infrequent endocytosis (thin arrow). Free cisternae of rough endoplasmic reticulum (RER), increased smooth endoplasmic reticulum (SER), and sinusoidal spaces (arrowhead) are also visible. D: demonstrates the presence of lipid droplets (LD) of variable density and intact microvilli (MV) in the very long sinusoidal spaces (arrowhead).

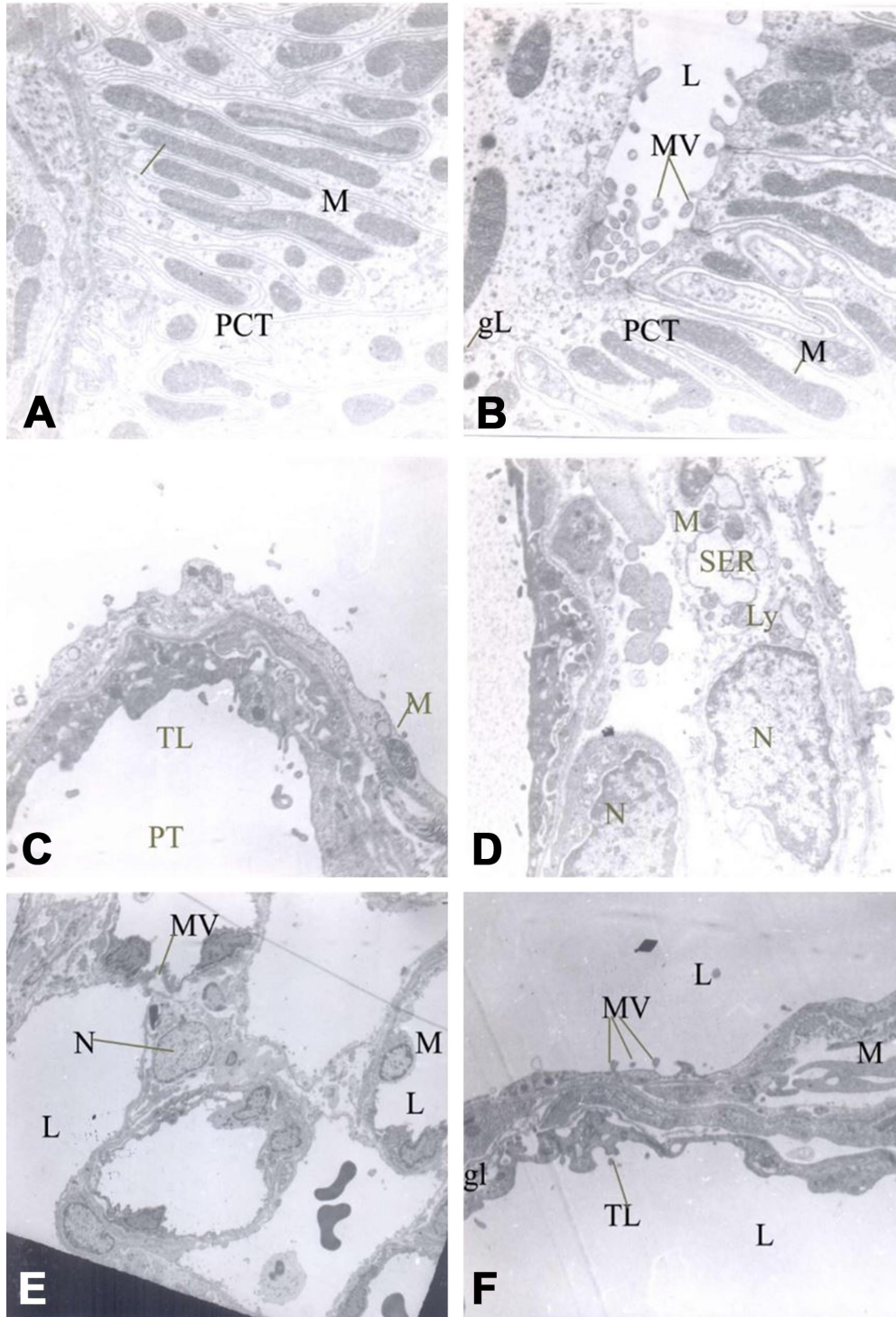


Fig. 3. A - Transmission electron micrograph (TEM) of ultrathin sections of the rat kidney. A: The electron micrograph of the S1 segment of the proximal convoluted tubule (PCT) illustrates a large number of dense mitochondria (M) among the intricate folding of the tubule. B: The S2 segment displays dense mitochondria (M) with occasional ruptures (thin arrow) and a lumen (L) featuring broken microvilli. C: An electron micrograph showcasing the proximal tubules (PT) reveals notable microvilli (Mv) (thin arrow). Additionally, observe the tubular lumen (TL) filled with necrotic debris (curled arrow). D: Limited number of mitochondria (M) with an electron-dense matrix. The nucleus (N) shows loss of chromatin condensation, and a few lysosomes (Ly) are also visible. Smooth endoplasmic reticulum (SER) with amorphous material is observed as well. E: treated kidney also showed lumen (L) with broken microvilli (Mv) and necrotic debris (F)

DISCUSSION

Our study reveals a notable decrease in body weight among rats treated with Etoposide in comparison to the control group. This observation aligns with the findings of previous investigation (Kamble *et al.*, 2013), which also demonstrated a significant reduction in body weight within the treated groups.

In this study, organ weights, including heart, kidney, and liver were assessed in the Etoposide model. No significant changes were observed in comparison with the control rats. However, our findings contrast with Ravindra *et al.* (2012) investigation who found significant changes in liver weight following treatment with 1.0 mg/kg i.p daily for 8 weeks. In Etoposide-treated rats, hepatic protein content did not show a significant increase. However, the total protein content in kidney and cardiac tissues significantly increased in comparison to controls. The drug treatment induced alterations in the total protein profiles of the organs. The alterations in protein levels may result from either the stimulated production of current or new proteins or from the destabilization and breakdown of existing proteins triggered by the drug.

The degradation of tissues and tissue fractions through lipid peroxidation is a process initiated by the generation and spread of free radical reactions, mainly engaging membrane polyunsaturated fatty acids. This phenomenon has been associated with the development of numerous diseases such as diabetes rheumatoid arthritis, atherosclerosis, and cancer, as well as complications like drug toxicity, aging, , and chemical reoxygenation injury (Halliwell & Gutteridge, 2015).

The assessment of malondialdehyde (MDA) concentration, serving as a marker for lipid peroxidation, was conducted in three organs. Elevated levels of end products from lipid peroxidation are commonly cited as a significant indicator of the association between free radicals and human diseases. Numerous studies substantiate the theory that the ingestion of lipid peroxidation products through food or their endogenous production poses a potential health hazard (Esterbauer *et al.*, 1993). Concerning Etoposide, it may induce lipid peroxidation in the liver, where free radicals generated by the drug play a role. Alternatively, it might occur in the liver, where cell membranes are less prone to oxidative harm induced by free radicals. This gives us probable indications that etoposide drug-induced oxidative stress is at a lower level in renal and cardiac tissues as compared to other tissues in rats.

Glutathione (GSH), a tripeptide featuring a reactive thiol group, holds a pivotal role as an antioxidant, combating

free radicals and various oxidants, while also serving a crucial function in the detoxification process. Its significance extends to the regulation of cell proliferation, restructuring of the extracellular matrix, modulation of mitochondrial respiration, facilitation of apoptosis, adjustment of redox signal transduction, and functioning as a reservoir for cysteine (Rahman & MacNee, 2000). The significant alteration of GSH activity inside the cell enhances the slight toxic effect of the drug (etoposide). This suggests that there is an increase in oxidative stress on tissues.

G-S-T showed increased levels in heart, kidney, liver and tissues, probably due to the fact that G-S-T acts as a detoxicating enzyme system as it brings about catalytic conjugation of the nucleophilic thiol group of glutathione with the electrophilic carbon atom. Our findings are consistent with those reported in (Mittal *et al.*, 2001) .

The activity of GR in cardiac, renal, and hepatic tissues was found to be considerably decreased in the etoposide-treated group, which perhaps hints that the oxidized glutathione is not converted to its reduced form for the process of biotransformation.

The data presented here indicates that the antioxidant enzyme parameter (GPx), investigated in the context of etoposide treatment on male rats, functions as a marker reflecting oxidative stress on tissues. GPx plays a role in breaking down H₂O₂ within cells and also transforms GSH into oxidized GSSG, as quantified by Rotuck *et al.* (1973). Similarly, GPx plays a critical role in maintaining redox status during acute oxidative stress because of its protective role in coordination with the antioxidant enzymes. The data obtained in our research agree with those reported by the authors (Yin *et al.*, 1998) .

Shirwarikar *et al.*, reported that catalase plays a significant role in the acquisition of tolerance to oxidative stress (Shirwaikar *et al.*, 2003) . Catalase is the only antioxidant enzyme that increases at both the mRNA and activity levels during human lung morphogenesis (Asikainen *et al.*, 1998). Perhaps the attack by free radicals and reactive oxygen species in anticancer drugs was high enough to increase the activity of catalase.

In the etoposide-treated group, the level of CYTp450 in hepatic and cardiac tissues presented a significant increase, whereas that in renal tissue showed an insignificant decrease as compared to controls. Higher levels of CYTp450 may have resulted in higher drug metabolism and vice versa. The lower concentration of CYTp450 was in accordance with our result (kidney) as reported by Nebert & Russell (2002).

In etoposide treatment, the level of CYT b5 shows significant depletion in cardiac, renal and hepatic tissues as compared with control. Perhaps a significant depletion in cytochrome b5 indicates the involvement of ROS in enzyme inactivation. Litterst *et al.* were unable to alter the levels of CYT p450 and b5 (Litterst *et al.*, 1983). Nebert & Russell (2002) report that CYTp450 and B5 play a very important role in the biotransformation and bioactivation of xenobiotics.

Histopathological examinations of the liver and kidney revealed various structural alterations following prolonged etoposide treatment. This aligns with findings from studies conducted by Kamble *et al.* (2013) and Ravindra *et al.* (2012), both of which documented structural changes in rats treated with etoposide.

CONCLUSION

The application of etoposide at the designated dosage and duration is likely to induce both structural and biochemical changes. Our results across biochemical, histological, and fine structural analyses align cohesively.

ACKNOWLEDGMENT. Researchers Supporting Project number (RSPD2024R757), King Saud University, Riyadh, Saudi Arabia.

KEWEDAR, S. M. R. & ABUTAHA, N. Cambios inducidos por el modelo de etopósido en estudios de antioxidantes, evaluaciones histológicas y ultraestructurales de tejidos hepáticos, renales y cardíacos de ratas macho. *Int. J. Morphol.*, 42(3):663-672, 2024.

RESUMEN: El etopósido es un agente antimitótico y antineoplásico eficaz que se utiliza para tratar diversas neoplasias malignas humanas. En el presente estudio, se inyectó etopósido por vía intraperitoneal a las ratas a razón de 1 mg/kg/día durante 52 días (52 dosis). Los animales control recibieron solución salina fisiológica (0,5 ml) por vía intraperitoneal diariamente por 52 dosis. El peso corporal de las ratas tratadas con etopósido se redujo significativamente en comparación con las ratas del grupo control. La peroxidación lipídica demostró un aumento insignificante del tejido hepático, una disminución no significativa del tejido renal y una reducción significativa del tejido cardíaco. Se encontró que los niveles de GSH en el tejido hepático y renal no aumentaron significativamente, pero sí aumentaron significativamente en el tejido cardíaco en comparación con los controles. Se encontró que la actividad de GR disminuyó considerablemente en el grupo tratado. Los niveles de G-S-T aumentaron significativamente en todos los grupos tratados. Las inyecciones de etopósido provocaron un cambio no significativo en el nivel de GPX del tejido hepático, mientras que los tejidos renal y cardíaco mostraron un aumento significativo. La actividad de CAT en el tejido hepático aumentó significativamente, mientras que la actividad de CAT en el tejido renal mostró una disminución no significativa, mientras que en el tejido cardíaco se observaron niveles significativamente más bajos

que en el grupo de control. El nivel de CYTp450 en los tejidos hepático y cardíaco mostró un aumento significativo; sin embargo, el tejido renal mostró un agotamiento no significativo, mientras que CYTb5 en los tejidos hepático, renal y cardíaco fue significativamente menor que los controles. El contenido de proteínas en el tejido hepático no aumentó significativamente, mientras que la proteína total en los tejidos renal y cardíaco aumentó significativamente. El hallazgo de la investigación es indicativo de la actividad de desintoxicación en el modelo de etopósido.

PALABRAS CLAVE: Etopósido; Antioxidante; Histológico; Ultraestructural; Hepático.

REFERENCES

- Asikainen, T. M.; Raivio, K. O.; Saksela, M. & Kinnula, V. L. Expression and developmental profile of antioxidant enzymes in human lung and liver. *Am. J. Respir. Cell Mol. Biol.*, 19(6):942-9, 1998.
- Baldwin, E. & Osheroff, N. Etoposide, topoisomerase II and cancer. *Curr. Med. Chem. Anticancer Agents*, 5(4):363-72, 2005.
- Esterbauer, H. & Cheeseman, K. H. Determination of aldehydic lipid peroxidation products: malonaldehyde and 4-hydroxynonenal. *Methods Enzymol.*, 186:407-21, 1990.
- Esterbauer, H.; Wäg, G. & Puhl, H. Lipid peroxidation and its role in atherosclerosis. *Br. Med. Bull.*, 49(3):566-76, 1993.
- Habig, W. H.; Pabst, M. J. & Jakoby, W. B. Glutathione S-transferases. The first enzymatic step in mercapturic acid formation. *J. Biol. Chem.*, 249(22):7130-9, 1974.
- Hadwan, M. H. & Abed, H. N. Data supporting the spectrophotometric method for the estimation of catalase activity. *Data Brief*, 6:194-9, 2016.
- Halliwell, B. & Gutteridge, J. M. *Free Radicals in Biology and Medicine*. Oxford, Oxford University Press, 2015.
- Hanauske, A. R.; Wüster, K. C.; Lehmer, A.; Rotter, M.; Schneider, P.; Kaeser-Fröhlich, A.; Rastetter, J. & Depenbrock, H. Activity of NK 611, a new epipodophyllotoxin derivative, against colony forming units from freshly explanted human tumours in vitro. *Eur. J. Cancer*, 31A(10):1677-81, 1995.
- Henwood, J. M. & Brogden, R. N. Etoposide. A review of its pharmacodynamic and pharmacokinetic properties, and therapeutic potential in combination chemotherapy of cancer. *Drugs*, 39(3):438-90, 1990.
- Kamble, P.; Kulkarni, S. & Bhiwgade, D. Ultrastructural and antioxidant studies of etoposide treated kidney of rat. *J. Cancer Sci. Ther.*, 5(4):137-41, 2013.
- Litterst, C. L.; Tong, S.; Hirokata, Y. & Siddik, Z. H. Stimulation of microsomal drug oxidation in liver and kidney of rats treated with the oncolytic agent cis-dichlorodiammineplatinum-II. *Pharmacology*, 26(1):46-53, 1983.
- Liu, L. F.; Liu, C. C. & Alberts, B. M. Type II DNA topoisomerases: enzymes that can unknot a topologically knotted DNA molecule via a reversible double-strand break. *Cell*, 19(3):697-707, 1980.
- Long, B. H. Mechanisms of action of teniposide (VM-26) and comparison with etoposide (VP-16). (VP-16). *Semin. Oncol.*, 19(2 Suppl. 6):3-19, 1992.
- Lowry, O. H.; Rosebrough, N. J.; Farr, A. L. & Randall, R. J. Protein measurement with the Folin phenol reagent. *J. Biol. Chem.*, 193(1):265-75, 1951.
- Mittal, A.; Pathania, V.; Agrawala, P. K.; Prasad, J.; Singh, S. & Goel, H. C. Influence of Podophyllum hexandrum on endogenous antioxidant defence system in mice: possible role in radioprotection. *J. Ethnopharmacol.*, 76(3):253-62, 2001.
- Moron, M. S.; Depierre, J. W. & Mannervik, B. Levels of glutathione, glutathione reductase and glutathione S-transferase activities in rat lung and liver. *Biochim. Biophys. Acta*, 582(1):67-78, 1979.

- Mross, K.; Hüttmann, A.; Herbst, K.; Hanauske, A. R.; Schilling, T.; Manegold, C.; Burk, K. & Hossfeld, D. K. Pharmacokinetics and pharmacodynamics of the new podophyllotoxin derivative NK 611. A study by the AIO groups PHASE-I and APOH. *Cancer Chemother. Pharmacol.*, 38(3):217-24, 1996.
- Nebert, D. W. & Russell, D. W. Clinical importance of the cytochromes P450. *The Lancet*, 360(9340):1155-62, 2002.
- Omura, T. & Sato, R. The carbon monoxide-binding pigment of liver microsomes. I. Evidence for its hemoprotein nature. *J. Biol. Chem.*, 239(7):2370-8, 1964.
- Racker, E. Glutathione reductase from bakers' yeast and beef liver. *J. Biol. Chem.*, 217(2):855-65, 1955.
- Rahman, I. & MacNee, W. Oxidative stress and regulation of glutathione in lung inflammation. *Eur. Respir. J.*, 16(3):534-54, 2000.
- Ravindra, P.; Kulkarni, S.; Dhume, C. & Bhiwgade, D. Histopathological and biochemical studies of etoposide treated liver of rat. *Int. J. Pharm. Bio Sci.*, 3(2):1-11, 2012.
- Rotruck, J. T.; Pope, A. L.; Ganther, H. E.; Swanson, A. B.; Hafeman, D. G. & Hoekstra, W. G. Selenium: biochemical role as a component of glutathione peroxidase. *Science*, 179(4073):588-90, 1973.
- Shirwaikar, A.; Malini, S. & Kumari, S. C. Protective effect of *Pongamia pinnata* flowers against cisplatin and gentamicin induced nephrotoxicity in rats. *Indian J. Exp. Biol.*, 41(1):58-62, 2003.
- Stähelin, H. F. & von Wartburg, A. The chemical and biological route from podophyllotoxin glucoside to etoposide: ninth Cain memorial Award lecture. *Cancer Res.*, 51(1):5-15, 1991.
- Weisel, G. F. Histology of the feeding and digestive organs of the shovelnose sturgeon, *Scaphirhynchus platorynchus*. *Copeia*, (3):518-25, 1979.
- Witterland, A. H.; Koks, C. H. & Beijnen, J. H. Etoposide phosphate, the water soluble prodrug of etoposide. *Pharm. World. Sci.*, 18(5):163-70 1996.
- Yin, X.; Wu, H.; Chen, Y. & Kang, Y. J. Induction of antioxidants by adriamycin in mouse heart. *Biochem. Pharmacol.*; 56(1):87-93, 1998.

Corresponding author:

Said M.R.Kewedar
Pennsylvania State University
State College
Pennsylvania
USA

E-mail: saeed.kewedar@gmail.com